NUMERICAL SIMULATIONS OF MULTIDIMENSIONAL FLOWS IN PRESENCE OF EITHER STRONG SHOCKS OR STRONG GRAVITATIONAL FIELDS

José A. Font[1], José Mª. Ibáñez[1], and José Mª. Martí[1,2]

RESUMEN

Se han obtenido algunas soluciones numéricas para describir flujos multidimensionales por medio de la *aproximación local por campos característicos*. Estas soluciones han sido utilizadas para poner a prueba un código bidimensional que extiende algunos *métodos de alta resolución de captura de ondas de choque*, diseñados recientemente para resolver sistemas hiperbólicos no lineales de leyes de conservación.

ABSTRACT

Some numerical solutions via local characteristic approach have been obtained describing multidimensional flows. These solutions have been used as tests of a two-dimensional code which extends some *high-resolution shock-capturing methods*, designed recently to solve nonlinear hyperbolic systems of conservation laws.

Key words: **HYDRODYNAMICS – BLACK HOLE – RELATIVITY – SHOCK WAVES**

1. INTRODUCTION

n the present paper we are reporting recent preliminary results in our project of developing a fully tivistic and multidimensional hydrodynamical code. Our main interest is to correctly model the formation propagation of strong shocks. The possible existence of a strong gravitational field, as a background in ch these shocks evolve, complicates the problem, and a fully general-relativistic description is necessary. trong shocks are present in several astrophysical scenarios: e.g., supernovae, accretion onto compact cts, jets (associated with either star formation or active galactic nuclei). A multidimensional description ecessary in order to understand the complex structures of these shocks when interacting with matter of interstellar or intergalactic medium or even more interestingly when dynamical instabilities of different ls are developed (for example Rayleigh-Taylor or Kelvin-Helmholtz) at the interfaces between two fluids. ally, a multidimensional analysis is necessary if we are interested in describing the release –even in a quasi-vtonian description– of gravitational radiation coming from the gravitational collapse of cores in evolved ssive stars or during the collision of two compact objects.

Vith this aim we have proposed, recently, an extension of the so-called *modern high-resolution shock-capturing* 10ds designed to solve nonlinear hyperbolic systems of conservation laws, which avoid the use of *artificial* 2sity to handle strong discontinuities. This has been applied to the relativistic hydrodynamics system of ations (Martí, Ibáñez, & Miralles 1991).

\ one dimensional *hyperbolic system of conservation laws* is:

$$\frac{\partial \mathbf{u}}{\partial t} + \frac{\partial \mathbf{f}(\mathbf{u})}{\partial x} = \mathbf{s}(\mathbf{u}) \quad , \tag{1}$$

ere u is the N-dimensional vector of unknowns and $f(u)$ are N-vector-valued functions called *fluxes*. Strictly aking a conservation law implies that the source term $s(u)$ is zero. The above system (1) is hyperbolic if Jacobian matrix

· Departamento de Física Teórica, Universidad de Valencia, Spain.
' Max-Planck-Institut für Astrophysik, Germany.

$$\mathbf{A} \;=\; \frac{\partial \mathbf{f(u)}}{\partial \mathbf{u}}$$

has real and distinct eigenvalues $\{\lambda_\alpha(u)\}_{\alpha=1,...N}$.

Our calculations have been classified in two sets:

1. Those involving a hyperbolic system of *linear* conservation laws in presence of strong gravitational fie (wave equation in a curved space-time).

In a series of papers (Petrich, Shapiro, & Teukolsky 1988 and Abrahams & Shapiro 1990) the relativis Euler and continuity equations have been formulated as a potential problem for some particular flo (irrotational, isentropic and perfect-fluid). The main advantage of this formulation has been the discovery analytic solutions simulating the steady-state accretion onto a Schwarzschild or Kerr gravitational field due a compact object. These solutions have, in our opinion, to be included in the list of tests to be considered builders of multidimensional relativistic codes. Although the potential flow prescription described in Petri et al. (1988) does not allow the presence of shock waves, for which the *shock-capturing methods* are particula indicated, we have considered that it would be interesting to apply these techniques to the problem at hai From the numerical point of view the interest of this application relies on the presence of non-linearit induced by the geometrical terms related to strong gravitational fields. From the astrophysical point of vie several authors have indicated that it would be worthwhile to apply these methods to the relativistic regii (see, for example Martí et al. (1991) and references therein).

2. Those involving a hyperbolic system of *nonlinear* conservation laws (Newtonian hydrodynamics).

In Martí (1991) a 1D code has been built which makes use of a Roe's linearization (see below for a revi of the Roe construction) for solving *local Riemann problems* at each interface of a given numerical grid.

A Riemann problem is an *initial value problem* for (1) with initial data:

$$\mathbf{u}(x,0) \;=\; \begin{cases} \mathbf{u_L} & if \; x \;<\; x_{shell} \\ \mathbf{u_R} & if \; x \;>\; x_{shell} \end{cases} \quad ,$$

where $u_{L,R}$ are, respectively, the left and right constant states of a given discontinuity at $x \;=\; x_{shell}$. general, the solution of that Riemann problem depends only on the states u_L, u_R and the ratio x/t.

This is what we call our MUSCL code (monotonic upstream schemes for conservation laws, Van Le (1979)).

The present paper is organized as follows: Section 2 is devoted to study some particular gener relativistic flows which can be described by a wave equation in a curved space-time. In § 3 we display t 2D Newtonian Euler equations of hydrodynamics and comment several aspects of interest concerning t numerical methods we are going to apply. The corner-stones of our numerical procedure are shown in § Particular attention has been paid to the Riemann solver derived by Roe in § 5. In § 6 we discuss the te underwent by our code. Finally, the main conclusions of our work are summarized in § 7.

2. GENERAL-RELATIVISTIC EQUATIONS FOR POTENTIAL FLOWS

For the sake of clarity, let us summarize the main steps in the derivation of the analytical solution for t steady-state, subsonic accretion of a gas onto a *Schwarzschild black hole*.

The key assumptions are: i) The gas obeys the equation of state $p \;=\; \rho \propto n^2$, where ρ is the mass-enei density, p the pressure and n the baryonic number density (we are using geometrized units: $c = G = 1$). The flow is made of a perfect fluid of null vorticity.

As a consequence of ii), a potential ψ exists such that the velocity field can be derived from it:

$$h u_\mu = \frac{\partial \psi}{\partial x^\mu} \quad ,$$

where $h \equiv (\rho + p)/n$ is the specific enthalpy and $u^\mu = (u^0, \mathbf{u})$ the four-velocity of the fluid. The equation continuity and assumption i) lead, finally, to a wave equation for the potential ψ in a curved space-time:

$$\psi^{;\mu}_{;\mu} = 0 \quad ,$$

re ; stands for the usual covariant derivative.

n the Schwarzschild gravitational field generated by a source of mass M this equation reads

$$\frac{\partial}{\partial r}\left[\left(1 - \frac{2M}{r}\right)r^2\frac{\partial\psi}{\partial r}\right] + \frac{1}{r^2}\left[\frac{1}{sin\theta}\frac{\partial}{\partial\theta}\left(sin\theta\frac{\partial\psi}{\partial\theta}\right) + \frac{1}{sin^2\theta}\frac{\partial^2\psi}{\partial\phi^2}\right] - \left(1 - \frac{2M}{r}\right)^{-1}\frac{\partial^2\psi}{\partial t^2} = 0 \qquad . \quad (5)$$

stationary solution of this equation which verifies the appropriate boundary conditions: i) finiteness of d h at the horizon of the black hole, ii) stationary flow into the source of the gravitational field, and iii) ymmetry, is

$$\psi = -u_\infty^0 t - 2Mu_\infty^0 ln(1 - 2M/r) + u_\infty(r - M)cos\theta \quad , \quad (6)$$

g u_∞^0 and u_∞ the asymptotic values of, respectively, the temporal component of the four-velocity and modulus of the three-vector u. Let us notice the following relations between u_∞^μ and the three-velocity or v_∞

$$u_\infty^\mu = (u_\infty^0, u_\infty) = (1 - v_\infty^2)^{-1/2}(1, v_\infty) \quad , \quad (7)$$

re v_∞ is the magnitude of the asymptotic fluid three-velocity. From the above solution for ψ the behavior ie velocity field is derived in a simple way (see equation (3)).

/e have solved the above wave equation (5) in the two-dimensional Schwarzschild's background by ting it into a system of three equations of first order. With this aim let us introduce the following rmediate functions

$$a = \frac{\partial\psi}{\partial t} \quad b = \frac{\partial\psi}{\partial r} \quad c = \frac{\partial\psi}{\partial\theta} \quad . \quad (8)$$

he first order system equivalent to (5) can be written as a hyperbolic system of conservation laws like the m (1) but in the two-dimensional space spanned by the independent variables r and θ

$$\frac{\partial u}{\partial t} + \frac{\partial f(u)}{\partial r} + \frac{\partial g(u)}{\partial\theta} = s(u) \quad , \quad (9)$$

re

$$u = (a, b, c) \quad (10)$$

e 3-dimensional vector of unknowns, and

$$f(u) = \left(-(1 - \frac{2M}{r})^2 b, -a, 0\right) \quad ,$$

$$g(u) = \left(-(1 - \frac{2M}{r})\frac{1}{r^2}c, 0, -a\right)$$

are the 3-vector-valued functions defining the *fluxes* in the r and θ directions, respectively. Finally

$$s(u) = \left(\left(1 - \frac{2M}{r}\right)\left(1 - \frac{3M}{r}\right)\frac{2}{r}b + \left(1 - \frac{2M}{r}\right)\frac{\cos\theta}{r^2\sin\theta}c, 0, 0 \right)$$

are the *source* terms.

In section § 4 we will analyse the properties of the above system (9) in the light of our numerical proce[..] for solving it.

3. 2D NEWTONIAN HYDRODYNAMICS

As a first step in our aim to design a multidimensional numerical code to deal with the equatio[..] relativistic hydrodynamics we will focus, in this section, on the Newtonian case. Just having avai[..] a multidimensional code which solves the Euler equations of Newtonian hydrodynamics and which [..] overcome severe numerical experiments is, in itself a very important task. Indeed, there are a lot of prob[..] in astrophysics relying on a correct numerical treatment of these equations (e.g., stellar winds, accr[..] flows, jets, stellar collapse). As we have pointed out at the introduction, the correct modelling of st[..] shocks and instabilities in multidimensional flows are the corner-stones of research in several areas of mo[..] astrophysics.

The governing equations of mass, momentum and energy for inviscid, plane, two-dimensional flow[..] as follows

$$\frac{\partial u}{\partial t} + \frac{\partial f(u)}{\partial x} + \frac{\partial g(u)}{\partial y} = 0 \quad,$$

where

$$u = (\rho, m, n, e)$$

is a 4-dimensional vector of unknowns,

$$f(u) = \left(m, \frac{m^2}{\rho} + p, \frac{mn}{\rho}, \frac{m}{\rho}(e+p) \right)$$

and

$$g(u) = \left(n, \frac{mn}{\rho}, \frac{n^2}{\rho} + p, \frac{n}{\rho}(e+p) \right) \quad;$$

with $m = \rho u$, $n = \rho v$, $e = \rho\left(\epsilon + (1/2)\left(u^2 + v^2\right)\right)$ where u and v are the x-component and y-component o[..] velocity field, and ρ and ϵ the density and internal energy, respectively. In addition, we assume that the[..] an equation of state of the form:

$$p = p(\rho, \epsilon) \quad.$$

The above equations represent the conservation of mass, momentum and energy, respectively.[..] equation of state closes the system.

In the next section we will review the properties of the above systems in the light of our nume[..] procedure to solve them.

4. NUMERICAL APPROACH

We have treated, from the numerical point of view, the above systems of equations (9) and (11) as hyperbolic systems of conservation laws and we have applied to them specific methods designed for such kind of problems (Martí et al. 1991).

4.1. *Our 1D algorithm*

For the sake of conciseness let us focus on the 1-D case. The basic ingredients of our algorithm are the following:

4.1.1. *Advancing in Time*

Let u_i^n be the cell-average of $\mathbf{u}$ over the cell i, having interfaces $x_{i-1/2}$ and $x_{i+1/2}$ and evaluated at time n. At the next time level, t^{n+1}, we have:

$$\mathbf{u}_i^{n+1} = \mathbf{u}_i^n - \lambda \left[\widehat{\mathbf{f}}(\mathbf{u}_i, \mathbf{u}_{i+1}) - \widehat{\mathbf{f}}(\mathbf{u}_{i-1}, \mathbf{u}_i) \right] + \Delta t \widehat{\mathbf{s}}_i(\mathbf{u}) \quad , \tag{16}$$

where $\lambda = \Delta t / \Delta x_i$, $\Delta t = t^{n+1} - t^n$ and $\Delta x_i = x_{i+1/2} - x_{i-1/2}$.

Let us notice that our numerical scheme has been written in *conservation form*. Lax & Wendroff (1960) showed that the limiting solution of any finite-difference scheme in conservation form is a weak solution. Harten, Lax, & Van Leer (1983) showed that, in the scalar case, *monotonic schemes* in conservation form always converge to the physically relevant solution. Finally, a practical advantage of writing a finite-difference scheme in conservation form is that the quantities that ought to be conserved, according to the differential equation, are exactly conserved in the difference form.

In order to gain accuracy in the temporal evolution, Runge-Kutta standard methods may be applied. To a system in two dimensions of the form

$$\frac{\partial \mathbf{u}}{\partial t} + \frac{\partial \mathbf{f}(\mathbf{u})}{\partial x} + \frac{\partial \mathbf{g}(\mathbf{u})}{\partial y} = 0 \tag{17}$$

would correspond a method of lines as

$$\frac{d\mathbf{u}_{i,j}(t)}{dt} = -\frac{\widehat{\mathbf{f}}_{i+\frac{1}{2},j} - \widehat{\mathbf{f}}_{i-\frac{1}{2},j}}{\Delta x} - \frac{\widehat{\mathbf{g}}_{i,j+\frac{1}{2}} - \widehat{\mathbf{g}}_{i,j-\frac{1}{2}}}{\Delta y} \quad , \tag{18}$$

where

$$\widehat{\mathbf{f}}_{i+\frac{1}{2},j} = \mathbf{f}(\mathbf{u}_{i-k,j}, \mathbf{u}_{i-k+1,j}, ..., \mathbf{u}_{i+k,j}) \tag{19}$$

and

$$\widehat{\mathbf{g}}_{i,j+\frac{1}{2}} = \mathbf{g}(\mathbf{u}_{i,j-k}, \mathbf{u}_{i,j-k+1}, ..., \mathbf{u}_{i,j+k}) \tag{20}$$

are the *numerical fluxes* (see below).

4.1.2. *Cell Reconstruction*

To obtain interface values from the cell-averaged quantities, u_i^{n+1}, different interpolation techniques have been used (Colella & Woodward 1984; Van Leer 1977, 1979). The order of the interpolation depends on the degree of spatial accuracy one wants to achieve. Usually a linear reconstruction has been used in most of our applications.

4.1.3. Numerical Fluxes

The numerical fluxes, $\hat{f}$, are evaluated by extending the numerical fluxes of Roe's first order upwind method (Roe 1981) for nonlinear scalar hyperbolic conservation laws to systems, via a *local characteristic approach* (Yee 1986). Roe's prescription can be applied to each one of the scalar uncoupled equations. In this way, the numerical fluxes can be written in terms of the original variables as

$$\hat{f}(u_L, u_R) = \frac{1}{2}\left(f_L + f_R - \sum_{\alpha=1}^{3} \mid \tilde{\lambda}_\alpha \mid \Delta\tilde{\omega}_\alpha\tilde{e}_\alpha\right) \quad , \tag{21}$$

where L and R stand for the left and right states of a given interface. $\tilde{\lambda}_\alpha$ and $\tilde{e}_\alpha$ ($\alpha = 1,2,3$) are the eigenvalues (*characteristic speeds*) and the eigenvectors of the Jacobian A, respectively, and the quantities $\Delta\tilde{\omega}_\alpha$ –the jumps of the local variables across each characteristic– are obtained from:

$$u_R - u_L = \sum_{\alpha=1}^{3} \Delta\tilde{\omega}_\alpha\tilde{e}_\alpha \quad ; \tag{22}$$

$\tilde{\lambda}_\alpha$, $\tilde{e}_\alpha$ and $\Delta\tilde{\omega}_\alpha$ as functions of u are evaluated at each interface and, therefore, they depend on the particular values u_L and u_R. The tilde $\sim$, stands for a particular average of the data of the problem.

Crucial to this local analysis is, then, the knowledge of the spectral decomposition of the Jacobian matrix of the system. For a more detailed description of the Roe construction see below.

4.1.4. Source Terms

The source terms $\hat{s}_i$ are obtained, to linear accuracy, from the values of the variables at the zone centers and at the previous time step.

Nevertheless, particular attention must be taken with the source terms, either in the case of stiff problems or in multidimensional applications. Several *time-splitting* algorithms allow to gain the accuracy required. An exact second order algorithm is the *Strang splitting* which can be written in an compact way

$$u^{n+1} = \mathcal{L}_s^{\Delta t/2}\mathcal{L}_f^{\Delta t}\mathcal{L}_s^{\Delta t/2}u^n \quad . \tag{23}$$

In (23) $\mathcal{L}_f$ is the operator in finite differences which solves the homogeneous part of system (1). On the other hand, $\mathcal{L}_s$ is the one that solves a system of ordinary differential equations of the form

$$\frac{\partial u}{\partial t} = s(u) \quad .$$

4.2. Extension to 2D problems

The multidimensional character of the systems (9) and (14) has been taken into account by considering standard *operator splitting* techniques. They are similar to the ones, explained before, used for treating the source terms.

The splitting proceeds in two steps and the algorithm can be written

$$u^{n+1} = \mathcal{L}_g^{\Delta t}\mathcal{L}_f^{\Delta t}u^n \quad , \tag{24}$$

where $\mathcal{L}_f$ and $\mathcal{L}_g$ stand for the operators in finite differences associated, respectively, to the 1D systems

$$\frac{\partial u}{\partial t} + \frac{\partial f(u)}{\partial x} = 0$$

d

$$\frac{\partial \mathbf{u}}{\partial t} + \frac{\partial \mathbf{g(u)}}{\partial y} = 0 \quad .$$

4.3. Jacobian Matrices and Spectral Decomposition

As we have emphasized before, crucial in our procedure is the knowledge of the spectral decomposition the Jacobian matrix of our system of partial differential equations.

4.3.1. Wave Equation in Schwarzschild Space-time

In this case the Jacobian matrices are, trivially, the identity matrix exception made of geometrical factors.

1. *r-direction*. The eigenvalues of the Jacobian matrix associated to the flux in the r-direction are

$$\lambda^0 = 0, \quad \lambda^\pm = \pm\left(1 - \frac{2M}{r}\right) \quad , \tag{25}$$

d the corresponding eigenvectors, $e_A(A = 0,\pm)$, have the components

$$\mathbf{e_0} = (0, 0, 1) \quad , \tag{26}$$

$$\mathbf{e_\pm} = \left(\mp\left(1 - \frac{2M}{r}\right), 1, 1\right) \quad . \tag{27}$$

2. *θ-direction*. The eigenvalues of the Jacobian matrix associated to the flux in the θ-direction are

$$\lambda^0 = 0, \quad \lambda^\pm = \pm\frac{1}{r}\left(1 - \frac{2M}{r}\right)^{1/2} \quad , \tag{28}$$

th the corresponding eigenvectors

$$\mathbf{e_0} = (0, 1, 0) \quad , \tag{29}$$

$$\mathbf{e_\pm} = \left(\mp\frac{1}{r}\left(1 - \frac{2M}{r}\right)^{1/2}, 0, 1\right) \quad . \tag{30}$$

4.3.2. 2D Newtonian Hydrodynamics (planar symmetry)

1. *Jacobian matrices*. Two Jacobian matrices (2) can be associated to each one of the fluxes appearing in 1).

It is worthwhile to introduce the following quantities

$$H = \frac{p + e}{\rho} \quad , \tag{31}$$

e fluid speed

$$q^2 = u^2 + v^2 \quad , \tag{32}$$

and the sound speed

$$c_s^2 = \chi + (p/\rho^2)\kappa \quad ,$$

(33)

where we have used the shorthand notation:

$$\chi = \frac{\partial p}{\partial \rho} \quad , \quad \kappa = \frac{\partial p}{\partial \epsilon} \quad ,$$

and being the total energy density

$$e = \rho\epsilon + \frac{1}{2}\rho(u^2 + v^2) \quad .$$

(35)

x-direction. – The jacobian matrix, **A**, associated to the flux **f** in the x-direction is

$$\mathbf{A} = \begin{bmatrix} 0 & 1 & 0 & 0 \\ c_s^2 - u^2 - \kappa/\rho(H - q^2) & u(2 - \kappa/\rho) & -v\kappa/\rho & \kappa/\rho \\ -uv & v & u & 0 \\ -uH + uc_s^2 - u\kappa/\rho(H - q^2) & H - u^2\kappa/\rho & -uv\kappa/\rho & u(1 + \kappa/\rho) \end{bmatrix}$$

y-direction. – The jacobian matrix, **B**, associated to the flux **g** in the y-direction is

$$\mathbf{B} = \begin{bmatrix} 0 & 0 & 1 & 0 \\ -uv & v & u & 0 \\ c_s^2 - v^2 - \kappa/\rho(H - q^2) & -u\kappa/\rho & v(2 - \kappa/\rho) & \kappa/\rho \\ -vH + vc_s^2 - v\kappa/\rho(H - q^2) & -uv\kappa/\rho & H - v^2\kappa/\rho & v(1 + \kappa/\rho) \end{bmatrix}$$

2. *Eigenvalues and Eigenvectors*

x-direction.– The eigenvalues which diagonalize the matrix **A** are:

$$\lambda^0 = u \quad ,$$

(36)

which has multiplicity two, and

$$\lambda^{\pm} = u \pm c_s \quad .$$

The corresponding eigenvectors, $e_A(A = 1,2,\pm)$, have the components

$$\mathbf{e}_1 = \left(1, u, v, H - \frac{\rho c_s^2}{\kappa}\right) \quad ,$$

(37)

$$\mathbf{e}_2 = (0, 0, v, v^2) \quad ,$$

(38)

and

$$\mathbf{e}_{\pm} = \left(1, u \pm c_s, v, H \pm u c_s\right) \quad .$$
$$(39)$$

y-direction.– The eigenvalues which diagonalize the matrix **B** are:

$$\lambda^0 = v \quad , \tag{40}$$

which, as before, has multiplicity two, and

$$\lambda^{\pm} = v \pm c_s \quad .$$

The corresponding eigenvectors, $e_A (A = 1,2,\pm)$, have the components

$$\mathbf{e}_1 = \left(1, u, v, H - \frac{\rho c_s^2}{\kappa}\right) \quad , \tag{41}$$

$$\mathbf{e}_2 = \left(0, u, 0, u^2\right) \quad , \tag{42}$$

and

$$\mathbf{e}_{\pm} = \left(1, u, v \pm c_s, H \pm v c_s\right) \quad . \tag{43}$$

Let us note the fact that although the eigenvalue λ^0 has a degeneracy, the set of eigenvectors is complete and preserves the strictly hyperbolic character of the system.

5. ROE'S RIEMANN SOLVER

Given the importance of this seminal technique we are going to point out the main steps leading to the so-called *Roe's numerical flux.*

In 1D, for clarity, let $x_i = i \Delta x$ and $t_n = n \Delta t$ be a discretization of space and time, and let us denote by v_i^n a piecewise linear approximation to the exact solution of the following nonlinear system of conservation laws

$$\frac{\partial \mathbf{u}}{\partial t} + \frac{\partial \mathbf{f}(\mathbf{u})}{\partial x} = 0 \quad . \tag{44}$$

The difference approximation to (44) can be written in *conservation form* as

$$\frac{\mathbf{v}_i^{n+1} - \mathbf{v}_i^n}{\Delta t} + \frac{\widehat{\mathbf{f}}_{i+1/2} - \widehat{\mathbf{f}}_{i-1/2}}{\Delta x} = 0 \quad , \tag{45}$$

where $\widehat{f}_{i+1/2}$ is the *numerical flux.* A numerical scheme in conservation form is called an *upwind scheme* if it reduces to the method of characteristics when applied to a linear system and also satisfies the entropy condition.

Roe's method consists, basically, in solving a *Riemann problem* for the linear system which comes from the above nonlinear system (44) according to the following prescriptions:

In the first step of the Roe construction, the exact system (44) is approximated in each computational cell $(x_i, x_{i+1}) \times (t_n, t_{n+1})$ by a linear system

$$\frac{\partial \mathbf{u}}{\partial t} + \frac{\partial \mathbf{G(u)}}{\partial x} = 0 \quad , \tag{46}$$

where

$$\mathbf{G(u)} = \mathbf{f}_i + \mathbf{A}_{i+1/2}(\mathbf{u} - \mathbf{v}_i^n) \quad , \quad \mathbf{f}_i = \mathbf{f}(\mathbf{u}_i) \quad . \tag{47}$$

Here the Roe matrix $A_{i+1/2}$ is such that:

1. $f_{i+1} - f_i = A_{i+1/2}(u_{i+1} - u_i)$ for any u_i and u_{i+1}. This property together with the Rankine-Hugoniot jump relations, implies that the speed of the discontinuity and the jump through it are, respectively, some eigenvalue and eigenvector of the matrix $A_{i+1/2}$. This implies that stationary discontinuities are steady solutions of the numerical scheme.

2. $A_{i+1/2}$ has real eigenvalues and a complete set of right eigenvectors.

3. In the limit as u_{i+1} and $u_i \to u_0$ is

$$\mathbf{A}_{i+1/2}(\mathbf{u}_{i+1}, \mathbf{u}_i) \to \mathbf{A}(\mathbf{u}_0) = \left(\frac{\partial \mathbf{f}}{\partial \mathbf{u}}\right)_{\mathbf{u}=\mathbf{u}_0} \quad . \tag{48}$$

In the second step of the construction, we solve the linear Riemann problem for the system (46) with the initial data defined as v_i^n for $x < x_{i+1/2}$ and v_{i+1}^n for $x > x_{i+1/2}$. It can be easily solved by decomposing the system (46) into a set of uncoupled scalar linear equations. With this aim let us multiply the system (46) by the left eigenvectors of the matrix $A_{i+1/2}$ and solve each scalar linear equation exactly.

The solution $v_{i+1/2}$ of the above Riemann problem at $x = x_{i+1/2}$ is given by

$$\mathbf{v}_{i+1/2} = \mathbf{v}_i + \sum_{k,\lambda_k^{i+1/2}<0} C_k^{i+1/2} \mathbf{R}_k^{i+1/2} \quad , \tag{49}$$

where $\lambda_k^{i+1/2}$ and $R_k^{i+1/2}$ represent the eigenvalue and the corresponding eigenvector of $A_{i+1/2}$. $C_k^{i+1/2}$ is the decomposition coefficient of $(v_{i+1} - v_i)$ in the right eigenvector space as defined by the following relation

$$\mathbf{v}_{i+1} - \mathbf{v}_i = \sum_k C_k^{i+1/2} \mathbf{R}_k^{i+1/2} \quad . \tag{50}$$

The numerical flux $\widehat{f}_{i+1/2} = G(v_{i+1/2})$ is given by

$$\widehat{\mathbf{f}}_{i+1/2} = \mathbf{f}_i + \sum_{k,\lambda_k^{i+1/2}<0} \lambda_k^{i+1/2} C_k^{i+1/2} \mathbf{R}_k^{i+1/2} \tag{51}$$

after substituting the value of $v_{i+1/2}$ given by (49). By property (1), it is equivalent to

$$\widehat{\mathbf{f}}_{i+1/2} = \mathbf{f}_{i+1} - \sum_{k,\lambda_k^{i+1/2}<0} \lambda_k^{i+1/2} C_k^{i+1/2} \mathbf{R}_k^{i+1/2} \quad , \tag{52}$$

or, finally, to this more familiar expression

$$\widehat{\mathbf{f}}_{i+1/2} = \frac{1}{2}\left(\mathbf{f}_i + \mathbf{f}_{i+1} - \sum_k |\lambda_k^{i+1/2}| \, C_k^{i+1/2} \mathbf{R}_k^{i+1/2}\right) \quad . \tag{53}$$

Some comments are in order:

1. Since the scheme is based on a linear decomposition of the characteristic fields, one can apply different numerical schemes for each field.

2. The scheme is non-oscillatory in the sense that no new extrema are created for the linear systems or a single nonlinear conservation law. No numerical spurious oscillations contaminate the calculations.

3. The above construction gives a difference approximation of first-order accuracy and may admit entropy violating shocks. Transonic rarefactions may generate unphysical solutions; they are prevented by adding some artificial viscosity only at the sonic points (see, for example, Harten & Hyman 1983).

Let us summarize the main steps in Roe's procedure:

1. Obtain matrix $A_{i+1/2}$ as defined in (47).

2. Compute the eigenvalues $\lambda_k^{i+1/2}$ and $R_k^{i+1/2}$ and the eigenvectors $R_k^{i+1/2}$ of $A_{i+1/2}$.

3. Calculate the decomposition coefficients $C_k^{i+1/2}$ as defined by (50).

4. Finally, compute $\hat{f}_{i+1/2}$ and obtain v_i^{n+1} by (45).

6. TESTS OF THE CODE

We are going to comment on one test for each of the cases considered above. Let us point out that the main difference between systems (9) and (11) relies on the fact that system (9) does not allow the presence of shocks while system (11) does.

6.1. *Potential Flow Passing over a Black Hole*

We have used a time-dependent simulation paying attention on the convergence to a steady state.

6.1.1. *Computational Mesh*

The angular coordinate θ varies in the interval $0 \leq \theta \leq \pi$. We have taken 30 equally spaced angular zones in the above interval. Other options are, for example, to take an angular uniform mesh in the interval $-1 \leq cos\ \theta \leq 1$.

Due to the presence of the *event horizon* at $r = 2M$, one has to take care on the choice of the radial coordinate. As in Abrahams & Shapiro (1990) we have introduced the so-called *tortoise coordinate*

$$r_* = r + 2Mln\left(\frac{r}{2M} - 1\right) \quad . \tag{54}$$

Our discretization in r_* spans the interval $-8.0\ M \leq r_* \leq 711.71\ M$, that is $2.0134\ M \leq r \leq 700\ M$. We have employed a geometrical grid – of ratio 1.026 – with 120 radial zones. Once the discretization in r_* is made, a Newton-Raphson algorithm allows to obtain the corresponding discretization in r. In this way our radial mesh is fine enough near the horizon to minimize the numerical errors in this region.

6.1.2. *Initial Conditions*

We have evolved in time the following initial state

$$\psi = u_\infty rcos\theta \quad , \tag{55}$$

$$\psi_t = -\left\{\left(1 - \frac{2M}{r}\right)\left[1 + \left(1 - \frac{2M}{r}\right)\psi_r^2 + \frac{1}{r^2}\psi_\theta^2\right]\right\}^{1/2} \quad , \tag{56}$$

$$\psi_r = u_\infty cos\theta \quad , \tag{57}$$

and

$$\psi_\theta = -u_\infty rsin\theta \quad . \tag{58}$$

6.1.3. Boundary Conditions

At the horizon $(r = 2M)$, the inner boundary, the baryon number density must be regular. From the normalization condition for the potential ψ

$$n = (-\psi_{;\mu}\psi^{;\mu})^{1/2} \quad ,$$

(59)

it is simple to derive the following expression for the baryon number density

$$n = \left[\left(1 - \frac{2M}{r}\right)^{-1}\psi_t^2 - \left(1 - \frac{2M}{r}\right)\psi_r^2 - \frac{1}{r^2}\psi_\theta^2\right]^{1/2}$$
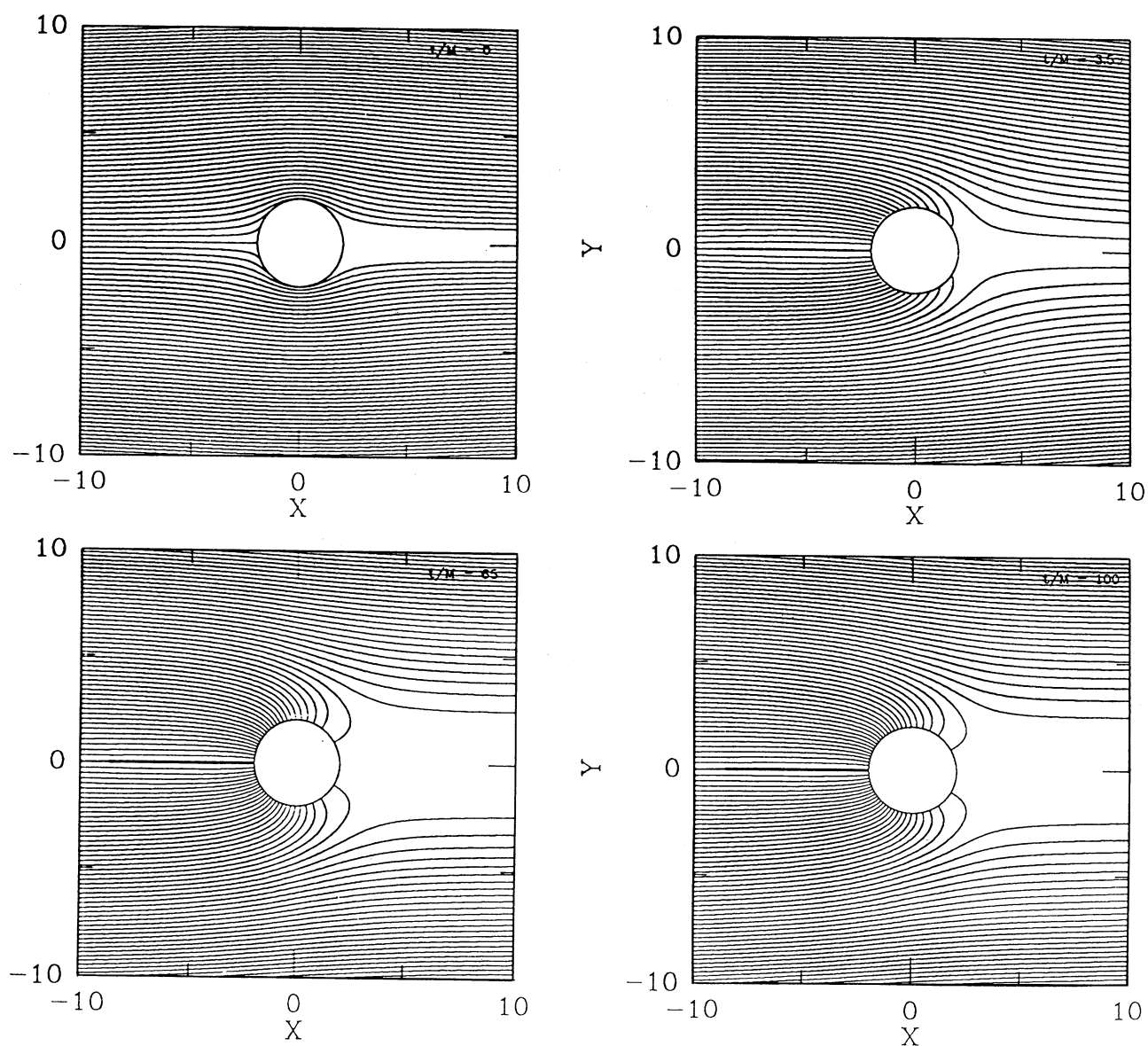
(60)

BLACK HOLE STEADY–STATE

Fig. 1a-1d. Evolution towards the steady-state accretion reached in a time $t \approx 65\ M$ for an asymptotic velocity $v_\infty^2 = 0.7$.

The regularity condition of n at the horizon requires that ψ_r diverges there in such a way as to cancel the singular term in ψ_t in the above equation. If we make an expansion of ψ_r about $r = 2M$:

$$\psi_{r_*} \equiv \left(1 - \frac{2M}{r}\right)\psi_r =$$

$$= \psi_t + a_1(t)(r - 2M) + a_2(t)(r - 2M)^2 + ... \tag{61}$$

Neglecting terms of order greater than two, we can, finally, write the following boundary condition at the horizon

$$\frac{\partial}{\partial r_*}\left[\frac{\psi_{r_*} - \psi_t}{r - 2M}\right] = 0 \quad . \tag{62}$$

At very long distances $(r \gg 2M)$ a constant asymptotic flow has been assumed.

6.1.4. Results

In Figures 1a–1d we can see the evolution towards the steady-state accretion reached in a time $t \approx 65$ t for an asymptotic velocity $v_\infty^2 = 0.7$. We have obtained a value of $3.42 \leq r_A/M \leq 3.95$ (this interval constrained by the resolution of our grid) for the radius of the critical cylinder inside which material is ultimately captured by the black hole (see last reference in Petrich et al. (1988) for an analytic expression), being the exact value $3.404\ M$ for an asymptotic velocity $v_\infty^2 = 0.7$. Our numerical result for the steady-state particle accretion rate agrees with the analytical one with an accuracy of 6%, when it is measured near the horizon.

The main conclusion from these figures is the following: we have succeeded in obtaining the stationary solution by using a second order method. These results encourage us to extend these methods to full 2-D general-relativistic hydrodynamics allowing, then, the simulation of strong shocks.

6.2. Emery's Step

A severe test for two-dimensional flows in the presence of shocks is the flat-faced step originally introduced by Emery (1968): a Mach 3 flow is injected into a tunnel containing a step. The tunnel is 3 units long and 1 unit wide. The step is 0.2 units high and is located 0.6 units from the left-hand end of the tunnel. Slab symmetry is assumed.

The boundary conditions are: 1) Reflecting boundary conditions along the walls of the tunnel and at the left face and the bottom of the step. 2) At the right and the left sides of the tunnel, respectively, outflow and inflow boundary conditions are applied.

The initial condition for the gas in the tunnel are given by

$$\rho(x, y, 0) = \rho_0 = 1.4 \quad ,$$

$$u(x, y, 0) = u_0 = 3 \quad ,$$

$$v(x, y, 0) = v_0 = 0 \quad ,$$

and

$$p(x, y, 0) = p_0 = 1$$

for all x, y.

The equation of state considered is the one of an ideal gas with $\gamma = 7/5$. Gas is continually fed in at the left-hand boundary with the flow variables given by $(\rho, u, v, p) = (\rho_0, u_0, v_0, p_0)$. A rectangular grid of 120 × 40 has been used.
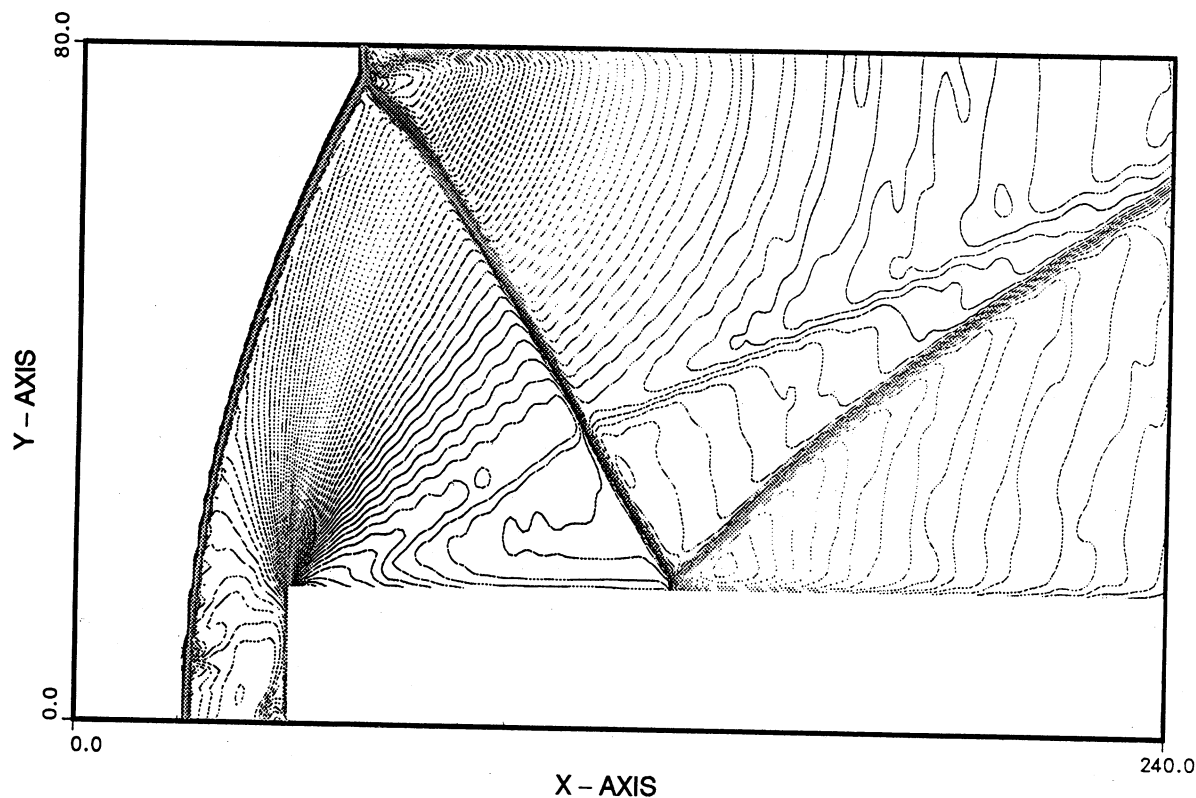
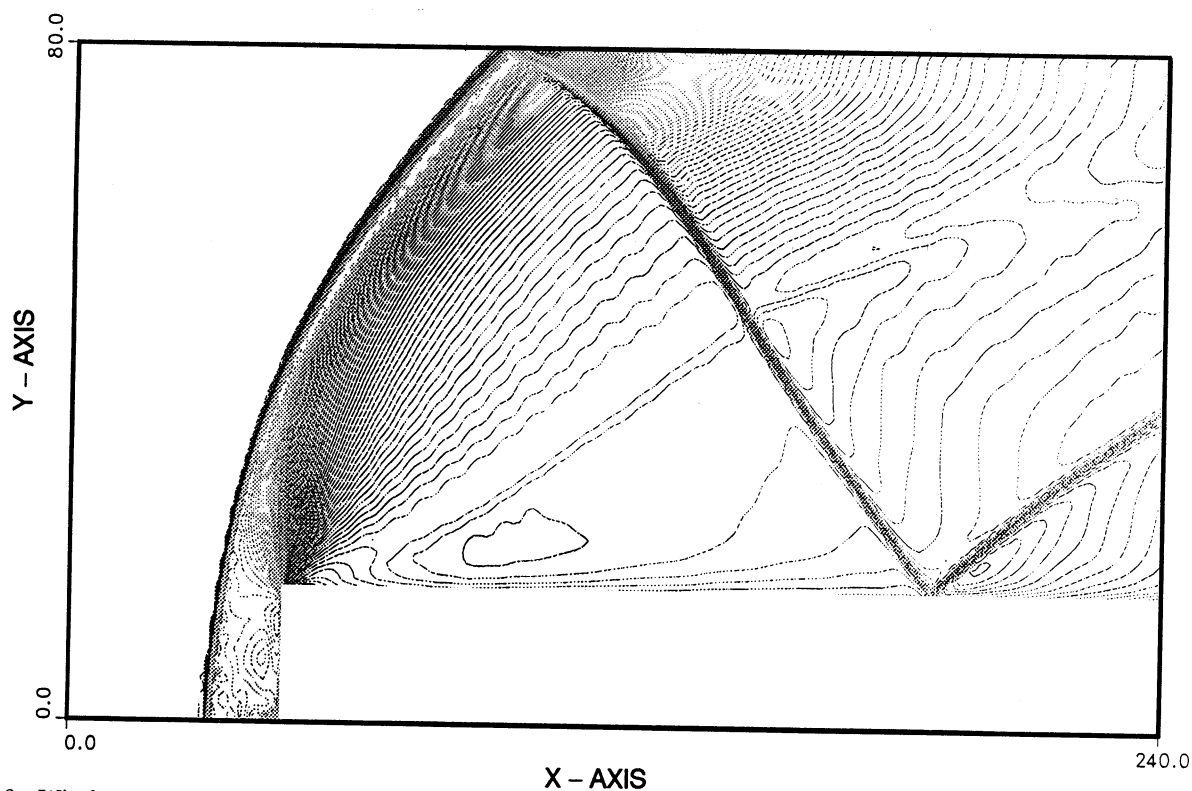Fig. 2. Emery s step: Isodensity contours at a time $t = 2.0$.

Fig. 3. Wind tunnel with a step. Same boundary conditions as in the Emery's step. Initial conditions are modified in order to have an inflow Mach number of 10. Isodensity contours at a time $t = 0.75$.

ιn operator splitting technique in each spatial direction in the sense of Strang (Yee 1989) has been formed. We have also experimented with methods which avoid the splitting in spatial directions and w advancing in time with a Runge-Kutta method (of third order in our case) such as we have explained ιre. In this last line of experimentation we have observed an important reduction of numerical noise and best results have been obtained.

ιt the transonic rarefactions, where entropy violation may appear (and, in fact, it does), a local artificial osity according to the prescription of Harten & Hymann (1983) was incorporated.

˙he main features of the solution are the Mach reflection of a *bow shock* on the upper wall, making the sity distribution the most difficult to compute, and a *rarefaction fan* centred at the corner of the step (see ιre 2).

˙he severity of this test makes us confident of the feasibility of astrophysical applications as complex as the s mentioned in the introduction of this paper.

˙oncerning this point let us make some comments: i) Obviously, the boundary conditions of this test are .cult to find in astrophysical scenarios. Nevertheless, the complex structure of the flow (e.g., bow shock, ɛction shock, rarefaction fan) makes this numerical experiment a challenging one in such a way that every .tidimensional hydrodynamical code should, in our opinion, overcome it. ii) In realistic flows we can ɛct Mach numbers higher than three. There is no problem for simulating them with the present version ur code. Figures 3 and 4 show the same experiment with increasing Mach numbers (10 and 100). We at present, analyzing these results, in particular those related with Figure 4, in order to be sure that the ιt breaking of the bow shock –roughly at the same altitude of the corner's step– is due to the high inflow ɩcity, to numerical diffusion or both. iii) Finally, we would like to point out –and we acknowledge some ιments of the referee– the fact that due to the symmetry of the problem, the same numerical experiment ιout the solid boundary walls at the top and bottom of the wind tunnel, might simulate a very dense jet pagating into a tenuous medium. The complex inner structure of the jet itself is, in this case, avoided.

X – AXIS
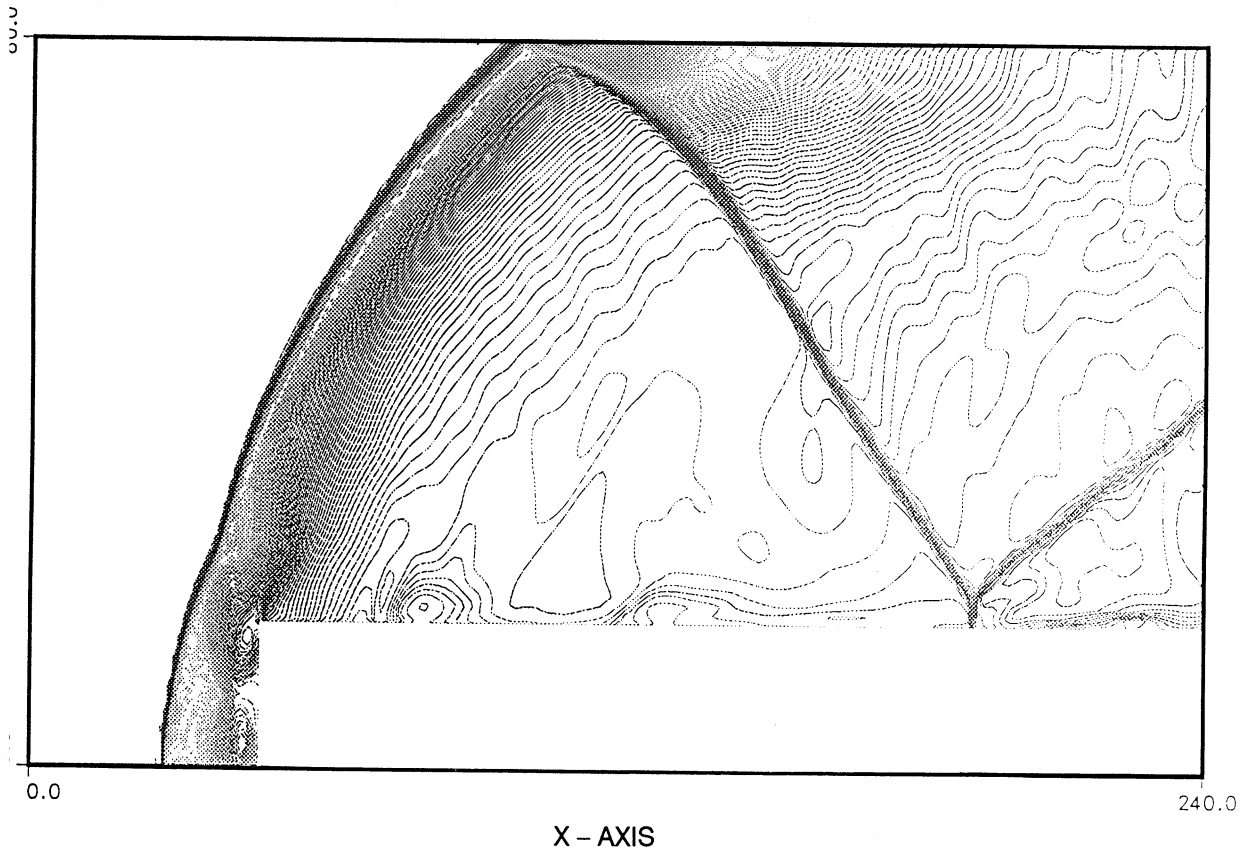
4. Wind tunnel with a step. Same boundary conditions as in the Emery's step. Initial conditions are modified in r to have an inflow Mach number of 100. Isodensity contours at a time $t = 0.1$.

7. CONCLUSIONS

The main conclusions from our applications are the following:

1. We have succeeded in obtaining stationary solutions of potential flows in a Schwarzschild backgrou That means that our 2D specific techniques together with the key algorithm which underlies our MUS code are robust enough to envisage other applications.

2. Minor modifications on the previous code have allowed us to deal with a very severe test in 2D N tonian hydrodynamics. Emery's step is a challenging test that every hydrodynamical code must overcom

The above conclusions will allow us to consider, with a dose of optimism, some of the astrophys applications already described. The basic ingredients for describing relativistic flows with or without sho with or without relativistic velocities and with or without strong gravitational fields, have been set up.

REFERENCES

Abrahams, A.M., & Shapiro, S.L. 1990, Phys. Rev., D 41, 327

Colella, P., & Woodward, P.R. 1984, J. Comp. Phys., 54, 174

Emery, A.F. 1968, J. Comp. Phys., 2, 306

Harten, A., & Hyman, J.M. 1983, J. Comp. Phys., 50, 235

Harten, A., Lax, P.D., & Van Leer, B. 1983, SIAM Rev., 25, 35

Lax, P.D., & Wendroff, B. 1960, Comm. Pure Appl. Math., 13, 217

Martí, J.M^a. 1991, Ph.D. Thesis, University of Valencia

Martí, J.M^a., Ibáñez, J.M^a., & Miralles, J.A. 1991, P Rev., D 43, 3794

Petrich, L.I., Shapiro, S.L., & Teukolsky, S.A. 1988, P Rev. Lett., 60, 1781

Roe, P.L. 1981, J. Comp. Phys., 43, 357

Van Leer, B. 1977, J. Comp. Phys., 23, 276

_____. 1979, J. Comp. Phys., 32, 101

Yee, H.C. 1986, in 10th International Conference Numerical Methods in Fluid Dynamics, eds. F.G. Z ang & Y.L. Zhu (Springer-Verlag)

_____. 1989, VKI Lecture Notes in Computational F Dynamics, (Belgium: von Karman Institute for F Dynamics)

José A. Font, José M^a. Ibáñez, and José M^a. Martí: Departamento de Física Teórica, Universidad de Vale 46100 Burjassot, Valencia, Spain.